Title

MEASUREMENTS OF STABILITY LIMITS FOR A SPACE-CHARGE-DOMINATED ION BEAM IN A LONG A.G. TRANSPORT CHANNEL

Authors

Tieferiback, M.G.
Keefe, D.

Publication Date

1985-05-01

LBL-19647

Lawrence Berkeley Laboratory
UNIVERSITY OF CALIFORNIA

Accelerator & Fusion Research Division

Presented at the 1985 Particle Accelerator Conference, Vancouver, B.C., Canada, May 13-16, 1985

MEASUREMENTS OF STABILITY LIMITS FOR A SPACE-CHARGE-DOMINATED ION BEAM IN A LONG A.G. TRANSPORT CHANNEL

M.G. Tiefenback and D. Keefe

May 1985

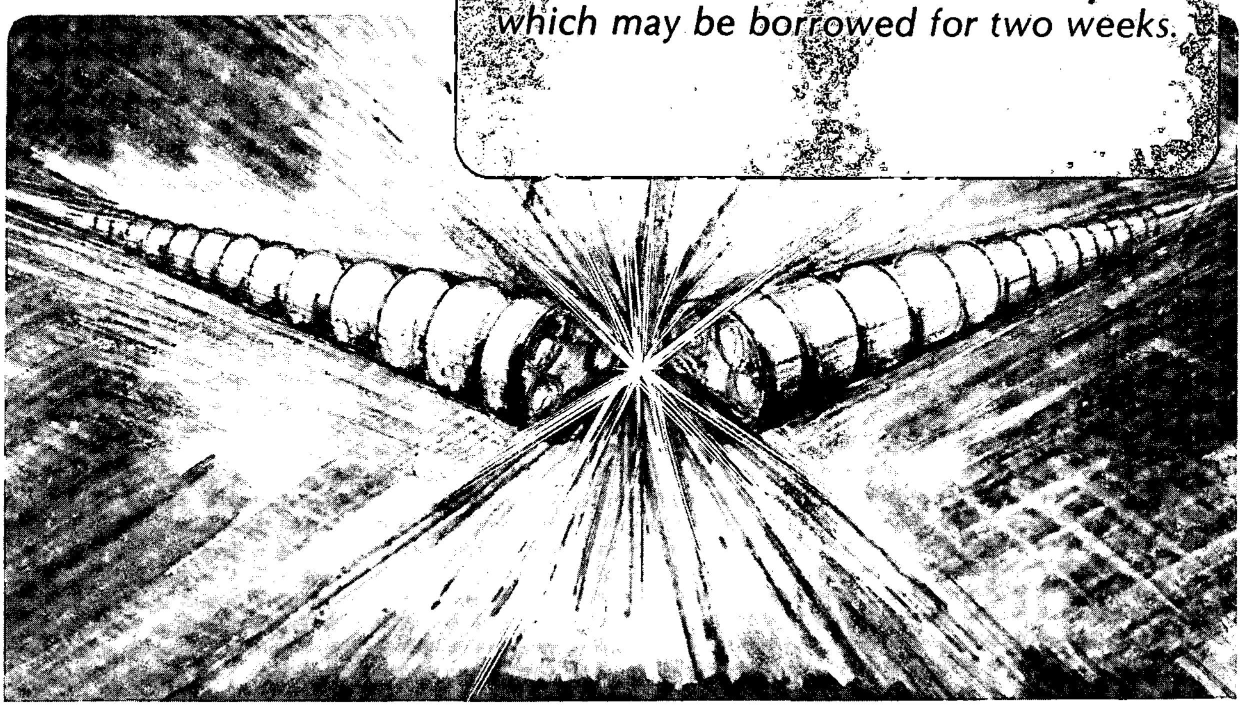

Prepared for the U.S. Department of Energy under Contract DE-AC03-76SF00098

LBL-19647
HIFAN-278

MEASUREMENTS OF STABILITY LIMITS FOR A SPACE-CHARGE-DOMINATED ION BEAM IN A LONG A.G. TRANSPORT CHANNEL*

M.G. Tiefenback and D. Keefe

Lawrence Berkeley Laboratory
University of California
Berkeley, CA 94720

May 1985

*This was supported by the Office of Energy Research, Office of Basic Energy Sciences, U.S. Department of Energy under Contract DE-AC03-76SF00098.

MACROSCOPIC QUANTUM EFFECTS IN THE ZERO VOLTAGE STATE OF THE CURRENT BIASED JOSEPHSON JUNCTION

John Clarke, Michel H. Devoret,* John Martinis, and Daniel Esteve*

Department of Physics, University of California and
Materials and Molecular Research Division
Lawrence Berkeley Laboratory
Berkeley, California, USA 94720

Introduction

Leggett (1-4) has stimulated interest in the question of whether quantum mechanics applies to macroscopic variables, an issue that has been addressed experimentally only recently. An attractive candidate for investigating this question is the Josephson tunnel junction (5), a system in which thermal fluctuations and perturbation due to the environment can be made relatively unimportant. In the case of the current-biased junction shown in Fig. 1(a), the macroscopic variable is the phase difference δ between the superconducting order parameters on either side of the barrier. For a model junction in which the complex impedance shunting the junction consists of a capacitance C and resistance R in parallel, the equation of motion for the junction is (6,7)

$$C(\Phi_0/2\pi)^2\ddot{\delta}+(1/R)(\Phi_0/2\pi)^2\dot{\delta}+(\Phi_0/2\pi)(\partial/\partial\delta)\{-I_0\cos\delta-[I+I_n(t)]\delta\} = 0, \quad (1)$$

where $\Phi_0 \equiv h/2e$ is the flux quantum. In general, both C and R may

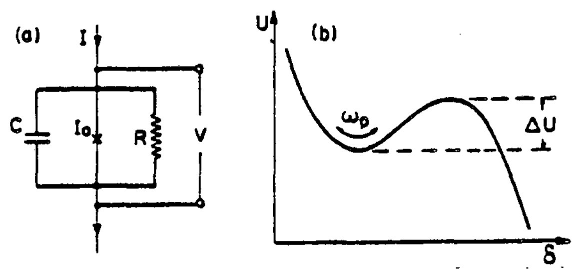

Fig. 1: (a) Resistively shunted junction model, and (b) U vs. δ for a bias current I below I_0.

contain contributions from the current-bias leads. We assume that R is independent of the voltage V across the junction. The critical current of the junction is I_o, the externally applied bias current is I, and the noise current due to Nyquist noise in the shunt resistance is $I_N(t)$. Equation (1) represents the motion of a particle moving in a one-dimensional tilted cosine potential. In the zero voltage state of the junction, the particle is confined to one well of this potential. After the particle escapes from this metastable state, it runs freely down the tilted washboard, and a voltage appears across the junction.

In the zero voltage state, the particle at the bottom of the well oscillates at the plasma frequency (1)

$$\omega_p(I) = \omega_{po}[1 - (I/I_o)^2]^{1/4} \qquad (I < I_o), \qquad (2)$$

where $\omega_{po} \equiv (2\pi I_o/C\Phi_o)^{1/2}$. The well is separated from the free running state by a potential barrier of height ΔU. In the limit of experimental interest the bias current is only slightly less than the critical current, and the potential from which the particle escapes becomes cubic [Fig. 1(b)]. In this approximation, the barrier height is (8)

$$\Delta U(I) = (4\sqrt{2}/3)U_o(1 - I/I_o)^{3/2} \qquad [(I_o - I)/I_o << 1], \quad (3)$$

where $U_o \equiv I_o\Phi_o/2\pi$. The dissipation is represented by the damping factor $Q = \omega_p RC$.

The mechanism by which the particle escapes from the metastable state is of central importance in the present context. In the thermal regime $k_BT >> \hbar\omega_p$, where T is the temperature, the noise current $I_N(t)$ in Eq. (1) adds a random force to the particle, which eventually escapes from the well by thermal activation at a rate proportional to (9) $\exp(-\Delta U/k_BT)$. On the other hand, in the quantum limit, the particle escapes by <u>macroscopic</u> <u>quantum</u> <u>tunneling</u> (MQT) (1-4) through the potential barrier. In the weak damping limit $Q >> 1$, and at $T = 0$ the predicted rate for this process is proportional to $\exp(-7.2\Delta U/\hbar\omega_p)(1 + 0.87/Q)$, where the first term in the exponent is the result of a WKB calculation (10) in the absence of any dissipation, and the second term arises from the effects of damping (1). The crossover temperature from the thermal regime to the quantum regime is predicted to be $T_o = \hbar\omega_p/2\pi k_B$ in the weak damping limit (11).

The experimental observation of MQT would imply that δ, which is a macroscopic variable in that it describes the phase difference between two large collections of Cooper pairs, obeys quantum mechanics. However, a quantitative demonstration of the correctness of the theoretical prediction may not be altogether trivial. A perusal of the equations listed above for the classical and quantum regimes reveals that the parameters governing the escape rate are I_o, C, R, I and T. Although one can, with care, expect to determine I and T with negligibly small error, the determination of I_o, C and R presents some difficulty. For example, because the plasma frequencies necessary to achieve the quantum limit are at least a few gigahertz (for millikelvin temperatures), and may be much higher, the impedance presented by leads coupled to the junction may have a major effect on the values of C and R that are to be used to compare the measured escape rates with theoretical predictions. It is necessary to understand these effects in some detail. A quite separate problem is concerned with possible effects of extraneous noise sources. As the temperature of the junction is lowered in the classical regime, the escape rate for fixed bias current drops rapidly. Below T_o, on the other hand, the escape rate is predicted to flatten off, as tunneling takes over from thermal activation. However, the presence of an extraneous noise source, for example pick-up from a radio or television station or Nyquist noise from a resistor at a temperature above that of the junction, may also cause the escape rate to flatten off as the temperature is lowered. Thus, one is required to demonstrate the absence of spurious effects of this kind. We shall return to these problems in due cause.

We now briefly mention experiments that were performed prior to those described in this paper. The escape rate in the thermal limit was measured by Fulton and Dunkleberger (8) in the ^{4}He temperature range using tunnel junctions with areas in the range of 4×10^{-3} to 10^{-4} mm^2. They reported "... lifetimes in near agreement with thermal-activation theory." The first measurements in the quantum regime were those of Voss and Webb (12) who studied 1 μm^2 tunnel junctions at temperatures down to 3 mK. They observed a flattening of the escape rate as the temperature was lowered that was consistent with the predictions of MQT for a junction with a high Q ($\beta_c \equiv 2\pi I_0 R^2 C/\Phi_0 = 5000$). On the other hand, for a lower Q junction ($\beta_c = 50$), a damping factor of approximately (1 + 5/Q) rather than (1 + 0.87/Q) was required to bring the low temperature escape rate into agreement with the theoretical prediction. However, the value of R used to determine Q was that obtained at low voltages from the I-V characteristic, whereas, as pointed out by the authors, "It is possible that the appropriate R ... is not the measured dc resistance near the origin but either the high-frequency resistance or the quasiparticle resistance above the gap." At about the same time, Jackel et al. (13) reported measurements on very small area tunnel junctions, with areas between 3×10^{-6} and 5×10^{-8} mm^2, in the ^4He temperature range. They also observed a flattening of the escape rate as the temperature was lowered, the flattening occurring at a lower temperature than one would predict from the theory in the absence of damping. They concluded that "The results are consistent with a prediction that dissipation reduces the rate of ... escape." Although both experiments in the quantum limit showed that the escape rate became independent of temperature as temperature was lowered and indicated that the presence of dissipation reduced the tunneling rate, it seems fair to say that in neither case were the parameters sufficiently well known to allow any quantitative comparison with theory to be made.

Experiments have also been performed on a different system, namely a superconducting loop interrupted by a Josephson tunnel junction [Fig. 2(a)]. In this case, one studies the thermal activation or quantum tunneling of the magnetic flux, Φ, threading the loop. For parameters of experimental interest, the potential $U(\Phi)$ contains two local minima, as indicated in Fig. 2(b). In the thermal regime, the particle hops between the two wells by thermal activation. One can determine the lifetime of the metastable state by ramping the applied flux and using a Superconducting QUantum Interference Device to determine when the transition between states occurs. Measurements in the thermal regime were made by Jackel et

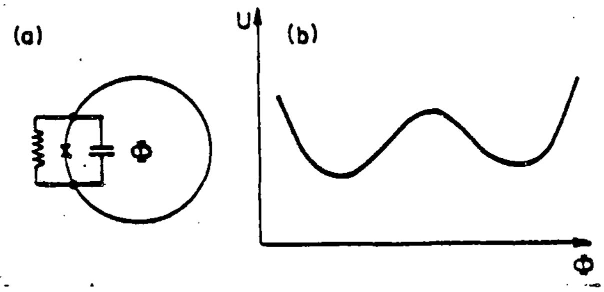

Fig. 2: (a) Superconducting ring interrupted by resistively shunted junction, and (b) U vs. Φ.

al. (14), using a point contact device in the ^{4}He temperature range. They concluded that "... the experimental results are in good agreement with the theory." In the quantum regime, Den Boer and de Bruyn Ouboter (15) also studied a point contact device in the ^{4}He temperature range, and observed that the transition rate between the two metastable states flattened off as the temperature was lowered. Prance et al. (16) [also Spiller et al. (17)] observed periodic structure in the V-I curve measured at radio frequencies on a tank circuit coupled to the loop containing a junction, and interpreted these results as arising from quantum effects. In both experiments in the quantum limit there appears to be uncertainty in the parameters of the point contact junctions, and the interpretation of the latter experiment has not been universally accepted (3). Very recently, Schwartz et al. (18) have studied a thin-film loop containing a Josephson tunnel junction that was heavily overdamped by means of an external shunt resistor. The junction area was about 0.1 μm^2, and measurements were made in the milliKelvin temperature range. They found good agreement with the predicted exponent of the tunneling rate, but a three-order-of magnitude discrepancy between the measured and predicted prefactor. The reasons for this discrepancy have yet to be understood.

The experiments described in the remainder of this paper are concerned with the escape rate from the zero-voltage state of a current-biased junction. The major difference between this work and previous experiments is that all of the relevant parameters of the junction are measured in situ using classical phenomena: in particular, we measure C and R at the relevant microwave frequencies. Thus, we are able to compare the experimental results with theoretical predictions with no adjustable parameters. We begin with a brief description of the experimental configuration. It is convenient, next, to describe the classical phenomenon of resonant activation from which we obtain ω_p and Q. We follow this with a description of the measurements of the escape rates in the thermal and quantum limits and compare our results with experimental predictions; at the same time, we describe the determination of I_0. The last experimental section is concerned with a different aspect of the quantum nature of δ, namely the quantization of the energy levels. We conclude with a brief summary.

Experimental Configuration

The junctions (19) were nominally $10 \times 10\ \mu m^2$ Nb-NbOx-Pb tunnel junctions fabricated in a cross-strip geometry on oxidized silicon wafers. The I-V characteristics exhibited a low subgap leakage current, and a diffraction-pattern-like modulation of the critical current as a function of the external magnetic field. Each junction in turn was attached to a custom-made attenuating coaxial line (mount) that was connected to the room temperature electronics via two coaxial lines, one for current and one for voltage, equipped with microwave and radiofrequency filters. The measured attenuation of the filters was greater than 150 dB from 0.1 to 12 GHz. A microwave current could be injected via a separate coaxial line, equipped with cold attenuators, that was capacitively coupled to the center conductor of the mount. For the experiments in the dilution refrigerator, the last of the chain of low-pass filters and the junction mount were attached to the mixing chamber. A magnetic field could be applied parallel to the plane of the junction by means of a superconducting magnet in the persistent current mode. The experiment and the battery-operated electronics required to operate it were enclosed in a screened room, with connections made to a microcomputer outside the room via fiber optics.

In all of the experiments except some of the resonant activation measurements, the escape rate $\Gamma(I)$ from the zero voltage state of the junction was determined using the method of Fulton and Dunkleberger (8) in which the bias current is ramped until the junction switches to a nonzero voltage. This voltage onset triggers an A-to-D converter monitoring the current, so that one obtains the value of current at which the junction switched. One repeats this procedure a large number of times, typically 10^5, to obtain the distribution of switching currents, P(I). The escape rate is calculated from the relation (8)

$$\Gamma(I) = \frac{P(I)dI/dt}{1 - \int_0^I P(i)di} . \qquad (4)$$

Resonant Activation

In resonant activation (19), one measures the lifetime $\tau(P)$ of the zero voltage state of the junction in the presence of a microwave power P. The microwave current is very small, and makes only a minor perturbation on the dynamics of the junction in the presence of thermal noise. The microwave current produces a sinusoidal force on the particle, so that one expects to observe a reduction in the lifetime of the metastable state when the microwave frequency is close to the plasma frequency. By measuring the resonant response of the lifetime to the microwaves, one is able to determine ω_p and Q and hence, knowing I and I_o, to deduce C and R.

To enable us to measure changes in $\tau(P)$ over a wide range of frequency, we measured τ directly at a fixed value of bias current while the microwave frequency was swept through the plasma resonance. In this method, we applied a 10 kHz square-wave modulated bias current and measured the time that elapsed between the leading edge of the pulse and the onset of a voltage across the junction in the absence of microwaves. To investigate the effect of microwaves, we injected a microwave current into the junction and swept the frequency. Although we observed a decrease in τ near the plasma frequency, the response exhibited a considerable amount of structure arising from variations in the attenuation of the line through which the microwaves were injected. We eliminated this problem by repeating the measurement at a slightly different value

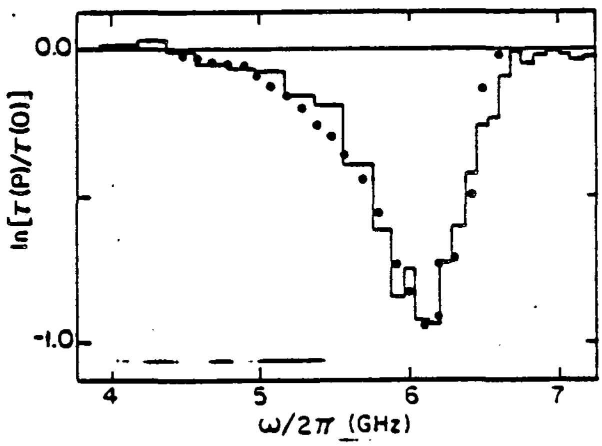

Fig. 3: Resonance in escape time vs. microwave frequency for junction in thermal limit at 4.2K with I_0 = 4.64 μA, Γ = 3.07 μA and τ(0) = 8.4 μs. Dots are experimental data and solid line is numerical simulation.

of I_0 (but the same value of I/I_0) so that the plasma frequency was shifted (in the example discussed here) by 0.12 GHz. Thus, the two curves differed significantly only in the plasma resonance, and by combining them we obtained the response of the junction at the average of the plasma frequencies. An example is shown in Fig. 3, where we plot ln[τ(P)/τ(0)] vs. microwave frequency for a junction at 4.2K.

In Fig. 3, we observe immediately that the lineshape is far from Lorentzian, having a much longer tail on the low frequency side of the peak than on the high frequency side. This non-Lorentzian lineshape arises from the fact that the oscillation frequency decreases as the energy of the particle in the cubic potential increases. To investigate this effect, we performed a numerical simulation of Eq. (1) with a sinusoidal driving current added to the bias and noise currents. The results of the simulation giving the best fit to the data are shown in Fig. 3, and mimic the asymmetry in the lineshape. The simulations indicate that the position of the minimum $\omega_m/2\pi$ is slightly less than $\omega_p/2\pi$, while the width $\Delta\omega/2\pi$ is somewhat larger than $\omega_p/2\pi Q$. The simulation shown in Fig. 3 is for ω_p = 6.3 GHz and Q = 13; for these values we find ω_m =

0.96 ω_p and $\Delta\omega = 1.25\ \omega_p/Q$. The inferred values of ω_p and Q lead to C = 6.8 pF and $R = Q/\omega_p C = 48\ \Omega$. The variations in the value of C due to the leads, about ± 0.5 pF, are a relatively small fraction of the junction capacitance, which was deliberately chosen to be as large as possible. On the other hand, the value of R is at least two orders of magnitude below the dynamic resistance determined from the I-V characteristic at low voltage. This value of R is determined entirely by the dissipation in the external circuitry.

We have seen that resonant activation enables one to determine the effective values of C and R _in situ_, provided one knows I_0 and I. In the next section we discuss the determination of I_0 and the measurement of the escape rate as a function of temperature.

Escape Rate in the Classical and Quantum Regimes

Escape temperature. In the thermal regime ($k_B T \gg \hbar\omega_p$) the thermally activated escape rate from the zero voltage state is predicted to be (20)

$$\Gamma_t = a_t(\omega_p/2\pi)\exp(-\Delta U/k_B T), \qquad (5)$$

where (20)

$$a_t = 4/[(1 + Qk_B T/1.8\Delta U)^{1/2} + 1]^2 \qquad (6)$$

is of the order of unity in our experiment. In the quantum regime ($k_B T \ll \hbar\omega_p$) to lowest order in 1/Q the macroscopic quantum tunneling rate out of the zero voltage state at T = 0 is predicted to be (1)

$$\Gamma_q = a_q(\omega_p/2\pi)\exp[-(7.2\Delta U/\hbar\omega_p)(1 + 0.87/Q)], \qquad (7)$$

where (1) $a_q = [120\pi(7.2\Delta U/\hbar\omega_p)]^{1/2}$.

To express the experimental results in a way that is as independent as possible of the junction parameters, it is convenient to introduce the _escape temperature_ T_{esc} defined through the relation

$$\Gamma = (\omega_p/2\pi)\exp(-\Delta U/k_B T_{esc}). \qquad (8)$$

In the thermal regime, the theoretical prediction is

$$T_{esc} = T/(1 - p_t) \qquad (k_B T >> \hbar\omega_p), \qquad (9)$$

where

$$p_t = (k_B T/\Delta U)\ln a_t \qquad (10)$$

is small compared with unity. In the quantum regime at T = 0, the prediction is

$$T_{esc} = \hbar\omega_p/k_B[7.2(1 + 0.87/Q)(1 - p_q)] \qquad (k_B T << \hbar\omega_p), \qquad (11)$$

where

$$p_q = (\hbar\omega_p/7.2\Delta U)\ln a_q. \qquad (12)$$

Determination of critical current. We determine I_0 in the thermal regime by using the exponential dependence of Γ_t on the bias current. As is evident from Eqs. (3) and (5), a plot of the experimentally determined quantity $\{\ln[\omega_p(I)/2\pi\Gamma(I)]\}^{2/3}$ vs. I should, neglecting departures of a_t from unity, be a straight line with slope scaling as $T_{esc}^{2/3}$ that intersects the current axis at I_0. As an illustration, we present results for a different 10 × 10 μm^2 junction to that represented in Fig. 2, incorporated in a different mount so that the external damping was reduced. Figure 4 shows three examples of such plots out of the seven obtained in the thermal regime over the temperature range from 102 to 800 mK. We also show two sets of data obtained at lower temperatures where quantum effects are expected to be important: we note that the slope changes very little as the temperature is lowered from 46 to 19 mK, indicating that T_{esc} is nearly the same at these two temperatures. As expected, the lines drawn through the data (using a least squares fit) intersect the current axis at very nearly the same point. The values of I_0 obtained from the seven sets of data in the thermal regime ranged from 9.498 to 9.535 μA. We then corrected these values of I_0 for the departure of a_t from unity, using the

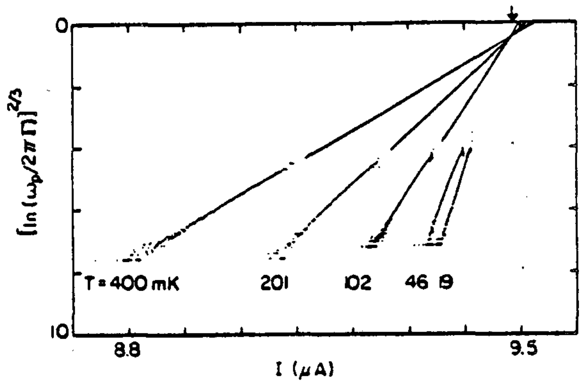

Fig. 4: $[\ln(\omega_p/2\pi\Gamma)]^{2/3}$ vs. I for five values of temperature. Lines that intersect the current axis have been drawn through the data in the thermal regime at the three highest temperatures. The arrow indicates the value of I_0 obtained after corrections for the prefactor were made.

value of Q = 30 ± 15 obtained from resonant activation. These corrections were small, ranging from -12 ± 4 na at 100 mK to -47 ± 12 nA at 800 mK. After these corrections were made, the critical current was independent of T to within the experimental uncertainties, with a value 9.489 ± 0.007 μA. Quantum corrections to I_0 in this temperature range were negligible.

From the values of $\omega_p(I)$ and Q(I) measured for three values of I_0 and numerous value of I we determined C and R as functions of ω_p. We found that our data were well explained by a lumped circuit model with C = 6.35 ± 0.4 pF and R = 190 ± 100 Ω.

Escape temperatures in thermal and quantum regimes. We used the measured values of I_0, R and C to calculate T_{esc} from Γ as a function of I and T. In Fig. 5 we plot (21) T_{esc} vs. T for a value of bias current such that $\ln(\omega_p/2\pi\Gamma) = 11$. The predicted crossover temperature of 30 mK is indicated by a solid arrow in Fig. 5. Above about 100 mK, T_{esc} is very close to T, as we expect in the thermal regime. Below about 25 mK, however, T_{esc} becomes independent of T, with a value of 37.4 ± 4 mK. The Caldeira-Leggett pre-

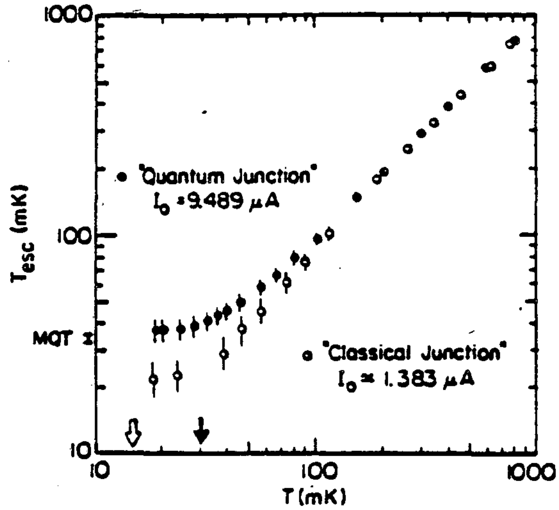

Fig. 5: T_{esc} vs. T for two values of critical current for $\ln(\omega_p/2\pi\Gamma) = 11$. The solid and open arrows indicate the predicted crossover temperatures for the higher and lower critical currents, respectively. Prediction of Eq. (5) for $I_0 = 9.489$ μA indicated at left.

diction (1) at T = 0 is $T_{esc} = 36.0 \pm 1.4$ mK, which is in very good agreement with the temperature-independent value observed in our experiment. The contribution of the damping to the predicted value of T_{esc} is -1.5 mK, which is less than the combined uncertainty of the prediction and experiment. Consequently, we cannot make any statement about the effect of dissipation on MQT.

Although the temperature-independent value of T_{esc} is in good agreement with the T = 0 prediction, nevertheless one should demonstrate that the flattening of T_{esc} is not due to an unknown, spurious noise source. To establish that the effective temperature of the dissipative element was equal to T at the lowest temperatures of the experiment, we reduced the critical current by means of a magnetic field so that the junction remained in the thermal limit. The critical current increased slightly as the temperature was lowered, from 1.376 ± 0.005 μA at 800 mK to 1.388 ± 0.002 μA at 20 mK. In Fig. 5 we have plotted T_{esc} for the lower critical current for $\ln(\omega_p/2\pi\Gamma) = 11$. At each temperature, we calculated T_{esc} using the measured value of I_0 at that temperature. The predicted crossover temperature, 14 mK, is indicated with an open arrow. We observe that T_{esc} is equal to T to within the experimental error over the entire temperature range, although there is a suggestion that T_{esc} is beginning to flatten off at the lowest temperature. We conclude that the flattening of T_{esc} for the junction with the higher critical current did not arise from spurious noise sources.

Quantization of Energy Levels

If the behavior of the particle in the well is determined by quantum mechanics, one would expect the energy of the particle to be quantized. To investigate this behavior, we have extended our measurements of the escape rate from the zero voltage state in the presence of a microwave current to the case where the junction is in the quantum regime. One expects the microwaves to enhance the escape rate when the frequency coincides with the spacing between two energy levels.

In the experiment (22), we adjusted the microwave power P so that $[\Gamma(P) - \Gamma(0)]/\Gamma(0) \lesssim 2$. We searched for resonances by varying the energy level spacing with the bias current while keeping the microwave frequency fixed. In Fig. 6(a) we show the escape rate vs. bias current in the presence of 2.0 GHz microwave irradiation for a $10 \times 80\ \mu m^2$ junction. The well contained several energy levels ($\Delta U/\hbar\omega_p \sim 6$), there was significant population of the lower excited states ($k_BT/\hbar\omega_p \sim 0.3$), and the damping was low ($Q \sim 80$). We observe three peaks in $[\Gamma(P) - \Gamma(0)]/\Gamma(0)$ that are characteristic of transitions between quantized energy levels. The two peaks at the higher bias currents are approximately Lorentzian. To investigate the positions of these peaks, we computed the energy levels by solving the Schrödinger equation numerically using the measured values of I, I_o and C. The solid lines in Fig. 6(b) represent the energy level spacings $E_{n\to n+1}$ vs. I ($n = 0,1,2$). The dotted lines represent the uncertainty in the $E_{0\to 1}$ curve due to the errors in I_o and C. We note that a given error in I_o and C will move all three curves by essentially the same amount. The intersection of each curve with the horizontal line corresponding to a microwave frequency of 2.0 GHz is the prediction of the value of bias current at

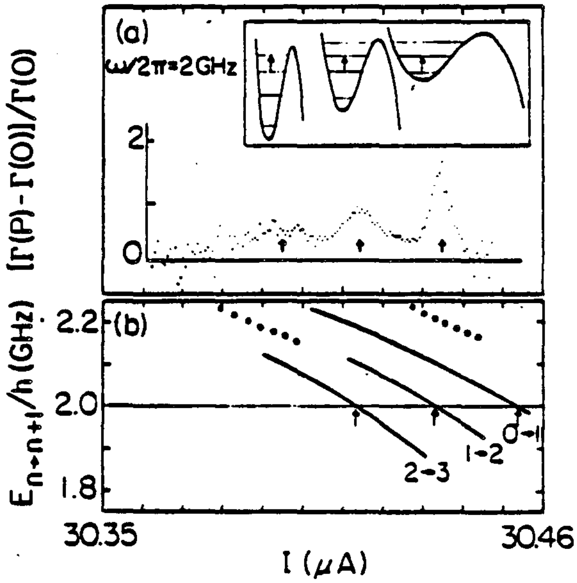

Fig. 6: (a) $[\Gamma(P) - \Gamma(0)]/\Gamma(0)$ vs. I for a 80 μm × 10 μm junction at 28 mK in the presence of 2.0 GHz microwaves ($k_BT/\hbar\omega$ = 0.29). Arrows indicate positions of resonances. Inset represents the corresponding transitions between energy levels. (b) Calculated energy level spacings $E_{n\to n+1}$ vs. I for I_0 = 30.572 ± 0.017 μA and C = 47.0 ± 3.0 pF. Dotted lines indicate uncertainties in the $E_{0\to 1}$ curve due to errors in I_0 and C. Arrows indicate values of bias current at which resonances are predicted.

which the resonant peaks should occur. The absolute positions of the measured peaks along the bias-current axis agree with the predictions to within the experimental uncertainties. The separations of the measured and predicted peaks are in excellent agreement.

To study the dependence of the separation ($E_1 - E_0$) on bias current, we have made measurements on a 10 × 10 μm^2 junction that was more strongly in the quantum regime ($k_BT/\hbar\omega$ ~ 0.1, $\Delta U/\hbar\omega_p$ ~ 2) at the experimentally accessible values of I and T. The values of I_0 and C were measured in the thermal regime in the usual way. Figure 7(a) shows the resonances observed at 18 mK for four different microwave frequencies, while Fig. 7(b) shows the values of the bias current at which the resonances are predicted to occur, together

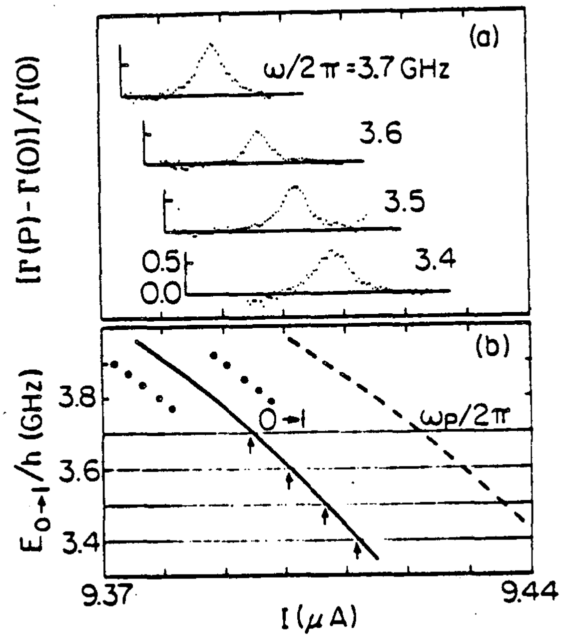

Fig. 7: (a) $[\Gamma(P) - \Gamma(0)]/\Gamma(0)$ vs. I for a 10 μm × 10 μm junction at 18 mK for four microwave frequencies. (b) Calculated energy level spacing $E_{0\to1}$ vs. I for I_o = 9.489 ± 0.007 μA and C = 6.45 ± 0.4 pF. Dotted lines indicate uncertainties due to errors in I_o and C. Arrows indicate values of bias current at which resonances are predicted. Dashed line indicates plasma frequency.

with the uncertainty. The absolute positions of the measured and predicted peaks agree to within the experimental uncertainties. The shift in the position of the resonances as the microwave frequency is changed is in excellent agreement with the predicted shift. We note that the measured positions of the resonances are very different from those that would be predicted classically for the resonant activation of a particle oscillating at the plasma frequency (dashed line).

As a final illustration, in Fig. 8 we show the evolution from quantum to classical behavior. At the lowest value of $k_BT/\hbar\omega$, the response is a single, approximately Lorentzian resonance. At a higher value of $k_BT/\hbar\omega$ a shoulder corresponding to the $E_{1\to2}$ transition becomes apparent. At the highest value of $k_BT/\hbar\omega$ the resonance is

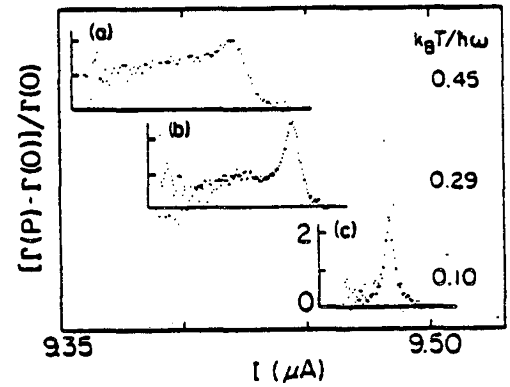

Fig. 8: $[\Gamma(P) - \Gamma(0)]/\Gamma(0)$ vs. I for the junction of Fig. 7 with I_0 = 9.57 μA and C = 6.35 pF at three values of $k_BT/\hbar\omega$. The microwave frequencies are (a) 4.5 GHz, (b) 4.1 GHz and (c) 3.7 GHz.

asymmetric, the peaks associated with individual transitions having merged into a continuum: this response is essentially classical.

To conclude this section, we comment briefly on the linewidth of the resonances. Resonant activation measurements in the classical limit for the junction illustrated in Fig. 7 yield Q = 30 ± 15. In the quantum limit, one expects the relative linewidth $\Delta\omega/\omega$ of the resonance corresponding to the $E_{0\to1}$ transition to be approximately 1/Q. The data presented in Fig. 7(a) yield $\omega/\Delta\omega$ = 50 ± 10, in reasonable agreement with the value of Q measured in the classical limit. We note that the coherence of the ground and excited states must be maintained over the lifetime of the excited state, approximately $2\pi Q/\omega_p$ ~ 14 ns; for the same transition in Fig. 6(a), the coherence time is about 40 ns.

Concluding Summary

When a weak microwave current is applied to a current-biased Josephson tunnel junction in the thermal limit the escape rate from the zero voltage state is enhanced when the microwave frequency is near the plasma frequency of the junction. The resonance curve is markedly asymmetric because of the anharmonic properties of the potential well: this behavior is well explained by a computer simulation using a resistively shunted junction model. This phenomenon of resonant activation enables one to make in situ measurements of the capacitance and resistance shunting the junction, including contributions from the complex impedance presented by the current leads. For the relatively large area junctions studied in these experiments, the external capacitive loading was relatively unimportant, but the damping was entirely dominated by the external resistance.

The values of C and R obtained from resonant activation together with the value of I_0 obtained from the current-dependence of the escape rate in the classical limit and the measured values of I and T completely specify the escape rate from the zero voltage state. This escape rate can be conveniently expressed as an escape temperature. As the temperature of the junction was lowered in the thermal regime, the escape temperature at a fixed value of ω_p/Γ was equal to the bath temperature to within the experimental error. At the lowest temperatures, however, the escape temperature flattened off to a value that was in excellent agreement with the Caldeira-Leggett prediction for $T = 0$ with no fitted parameters. For the junction reported here with $Q = 30$, the effects of damping were smaller than the experimental uncertainties, and it was not possible to draw any conclusions about the correctness of the prediction for the effects of dissipation on the macroscopic tunneling rate. As a check on the level of spurious noise, the measurements were repeated with the critical current reduced by a magnetic field so that the junction remained in the classical limit down to the lowest temperature of the experiment. The escape temperature remained close to the bath temperature over the entire temperature range, implying that external noise effects were negligible.

As a quite different demonstration of the quantum nature of δ, an experiment was performed to show that in the quantum limit the energy of the particle in the well is quantized. The escape rate from the zero voltage state was measured at constant microwave frequency and current as a function of the bias current. A peak in the escape rate was observed when, for example, the spacing between the ground state and first excited state coincided with the microwave frequency: the microwaves excite the particle from the ground state to the excited state in which the lifetime against tunneling out of the well is substantially reduced. At values of $k_BT/\hbar\omega$ such that there was a significant thermal population of the lower excited states, transitions between the n = 1 and n = 2 states and between the n = 2 and n = 3 states were also observed. The measured positions of the peaks were in excellent agreement with the predictions of a model calculation for the energy levels in the well, with no fitting parameters. The relative linewidth of the transition from the n = 0 to the n = 1 state was approximately 1/Q, as expected, and implied a coherence of the two states for periods up to 40 ns.

The observation of an escape rate from the zero voltage state of a junction in the quantum limit that is in excellent agreement with theoretical predictions together with the demonstration that the energy levels in the well are quantized provide extremely strong evidence that the macroscopic variable δ obeys quantum mechanics.

Acknowledgments

We are indebted to Claude Hilbert for a critical reading of the manuscript. This work was supported by the Director, Office of Energy Research, Office of Basic Energy Sciences, Materials Sciences Division of the U.S. Department of Energy under Contract No. DE-AC03-76SF00098. MHD and DE gratefully acknowledge partial support from the Commissariat a l'Energie Atomique.

References

*Permanent address: Service de Physique du Solide et de Résonance Magnétique, Centre d'Etudes Nucléaires de Saclay, 91191 Gif-sur-Yvette Cedex, France.

1. Caldeira, A.O., and A.J. Leggett. 1980. Annals of Physics 149, 374.
2. Leggett, A.J.. 1980. Prog. Theor. Physics (Suppl.) 69, 80.
3. Leggett, A.J.. 1984. In: Essays in Theoretical Physics in Honor of Dirk Ter Haar. Pergamon, New York, p. 95.

4. Leggett, A.J.. 1984. Contemp. Phys. 25, 583.

5. Josephson, B.D.. 1962. Phys. Lett. 1, 251.

6. Stewart, W.C.. 1968. Appl. Phys. Lett. 12, 277.

7. McCumber, D.E.. 1968. J. Appl. Phys. 39, 3133.

8. Fulton, T.A. and L.N. Dunkleberger. 1974. Phys. Rev. B 9, 4760.

9. Kramers, H.A.. 1960. Physica (Utrecht) 7, 284.

10. Ivanchenko, Yu.M. and L.A. Zilberman. 1968. Zh. Eksp. Teor. Fiz. 55, 2395 [1969. Sov. Phys. JETP 28, 1272].

11. Affleck, I.. 1981. Phys. Rev. Lett. 46, 388.

12. Voss, R.F. and R.A. Webb. 1981. Phys. Rev. Lett. 47, 647.

13. Jackel, L.D., L.P. Gordon, E.L. Hu, R.E. Howard, L.A. Fetter, D.M. Tennant, R.W. Epworth, and J. Kurijärvi. 1981. Phys. Rev. Lett. 47, 697.

14. Jackel, L.D., W.W. Webb, J.E. Lukens, and S.S. Pei. 1974. Phys. Rev. B 9, 115.

15. Den Boer, W. and R. de Bruyn Ouboter. 1980. Physics 98B, 185.

16. Prance, R.J., A.P. Long, T.D. Clark, A. Widom, J.E. Mutton, J. Sacco, M.W. Potts, G. Megaloudis, and F. Goodall. 1981. Nature 289, 543.

17. Spiller, T.P., J.E. Mutton, H. Prance, R.J. Prance, T.D. Clark, and R. Nest. 1985. These proceedings.

18. Schwartz, D.B., B. Sen, C.N. Archie, A.K. Jain, and J.E. Lukens. 1985. These proceedings.

19. Devoret, M.H., J.M. Martinis, D. Esteve, and J. Clarke. 1984. Phys. Rev. Lett. 53, 1260.

20. Buttiker, M., E.D. Harris, and R. Landauer. 1983. Phys. Rev. B 28, 1268.

21. Devoret, M.H., J.M. Martinis, and J. Clarke. 1985. (unpublished).

22. Martinis, J.M., M.H. Devoret, and J. Clarke. 1985. (unpublished).